Title: Detecting the impact of temperature on transmission of Zika, dengue and chikungunya using mechanistic models

Short title: Temperature predicts Zika, dengue, and chikungunya transmission

Authors: Erin A. Mordecai[a*], Jeremy M. Cohen[b], Michelle V. Evans[c], Prithvi Gudapati[a], Leah R. Johnson[b], Catherine A. Lippi[c], Kerri Miazgowicz[d], Courtney C. Murdock[d,e], Jason R. Rohr[b], Sadie J. Ryan[c,f,g,h], Van Savage[i,j], Marta S. Shocket[a,k], Anna Stewart Ibarra[l], Matthew B. Thomas[m], Daniel P. Weikel[n]

Affiliations:

[a]Biology Department, Stanford University, 371 Serra Mall, Stanford, CA 94305

[b]Department of Integrative Biology, University of South Florida, 4202 East Fowler Ave, SCA110 Tampa, FL 33620

[c]Department of Geography, University of Florida, PO Box 117315, Turlington Hall, Gainesville, FL 32611

[d]Center for Tropical and Emerging Global Disease, Department of Infectious Diseases, University of Georgia College of Veterinary Medicine, 501 D.W. Brooks Drive, Athens, GA 30602

[e]Odum School of Ecology, University of Georgia, 140 E. Green St., Athens, GA 30602[f]Emerging Pathogens Institute, University of Florida, P.O. Box 100009, 2055 Mowry Road Gainesville, FL 32610

[g]Center for Global Health and Translational Science, Department of Microbiology and Immunology, Weiskotten Hall, SUNY Upstate Medical University, Syracuse, NY 13210

[h]School of Life Sciences, College of Agriculture, Engineering, and Science, University of KwaZulu Natal, Private Bag X01, Scottsville, 3209, KwaZulu Natal, South Africa

[i]Department of Ecology and Evolutionary Biology, University of California Los Angeles and Department of Biomathematics, University of California Los Angeles, Los Angeles, CA 90095

[j]Santa Fe Institute, 1399 Hyde Park Rd, Santa Fe, NM 87501

[k]Department of Biology, Indiana University, 1001 E. 3rd St., Jordan Hall 142, Bloomington, IN 47405

[l]Center for Global Health and Translational Sciences, SUNY Upstate Medical University, Syracuse, NY13210

[m]Department of Entomology and Center for Infectious Disease Dynamics, Penn State University, 112 Merkle Lab, University Park, PA 16802

[n]Department of Biostatistics, University of Michigan, 1415 Washington Heights, Ann Arbor, MI 48109

[*]Correspondence to: Erin Mordecai. Biology Department, Stanford University, 371 Serra Mall, Stanford, CA 94305. (650) 497-7447. emordeca@stanford.edu

Keywords: Zika, dengue, chikungunya, temperature, vector transmission, *Aedes aegypti*, *Aedes albopictus*

Abstract

Recent epidemics of Zika, dengue, and chikungunya have heightened the need to understand the seasonal and geographic range of transmission by *Aedes aegypti* and *Ae. albopictus* mosquitoes. We use mechanistic transmission models to derive predictions for how the probability and magnitude of transmission for Zika, chikungunya, and dengue change with mean temperature, and we show that these predictions are well matched by human case data. Across all three viruses, models and human case data both show that transmission occurs between 18-34°C with maximal transmission occurring in a range from 26-29°C. Controlling for population size and two socioeconomic factors, temperature-dependent transmission based on our mechanistic model is an important predictor of human transmission occurrence and incidence. Risk maps indicate that tropical and subtropical regions are suitable for extended seasonal or year-round transmission, but transmission in temperate areas is limited to at most three months per year even if vectors are present. Such brief transmission windows limit the likelihood of major epidemics following disease introduction in temperate zones.

Author Summary (150-200 words)

Understanding the drivers of recent Zika, dengue, and chikungunya epidemics is a major public health priority. Temperature may play an important role because it affects mosquito transmission, affecting mosquito development, survival, reproduction, and biting rates as well as the rate at which they acquire and transmit viruses. Here, we measure the impact of temperature on transmission by two of the most common mosquito vector species for these viruses, *Aedes aegypti* and *Ae. albopictus*. We integrate data from several laboratory experiments into a mathematical model of temperature-dependent transmission, and find that transmission peaks at

26-29°C and can occur between 18-34°C. Statistically comparing model predictions with recent observed human cases of dengue, chikungunya, and Zika across the Americas suggests an important role for temperature, and supports model predictions. Using the model, we predict that most of the tropics and subtropics are suitable for transmission in many or all months of the year, but that temperate areas like most of the United States are only suitable for transmission for a few months during the summer (even if the mosquito vector is present).

Main Text

Epidemics of dengue, chikungunya, and Zika are sweeping through the Americas, and are part of a global public health crisis that places an estimated 3.9 billion people in 120 countries at risk [1]. Dengue virus (DENV) distribution and intensity in the Americas has increased over the last three decades, infecting an estimated 390 million people (96 million clinical) per year [2]. Chikungunya virus (CHIKV) emerged in the Americas in 2013, causing 1.8 million suspected cases from 44 countries and territories (www.paho.org). In the last two years, Zika virus (ZIKV) has spread throughout the Americas, causing 714,636 suspected and confirmed cases, with many more unreported (http://ais.paho.org/phip/viz/ed_zika_cases.asp, as of January 5, 2017). The growing burden of these diseases (including links between Zika infection and both microcephaly and Guillain-Barré syndrome [3]) and potential for spread into new areas creates an urgent need for predictive models that can inform risk assessment and guide interventions such as mosquito control, community outreach, and education.

Predicting transmission of DENV, CHIKV, and ZIKV requires understanding the ecology of the vector species. For these viruses the main vector is *Aedes aegypti*, a mosquito that prefers and is closely affiliated with humans, while *Ae. albopictus*, a peri-urban mosquito, is an important secondary vector [4,5]. We expect one of the main drivers of the vector ecology to be the climate, particularly temperature. For that reason, mathematical and geostatistical models that incorporate climate information have been valuable for predicting and responding to *Aedes* spp. spread and DENV, CHIKV, and ZIKV outbreaks [5–10].

The effects of temperature in ectotherms are largely predictable from fundamental metabolic and ecological processes. Survival, feeding, development, and reproductive rates predictably respond to temperature across a variety of ectotherms, including mosquitoes [11,12].

Because these traits help to determine transmission rates, the effects of temperature on transmission should also be broadly predictable from mechanistic models that incorporate temperature-dependent traits. Here, we introduce a model based on this framework that overcomes several major gaps that currently limit our understanding of climate suitability for transmission. Specifically, we develop models of temperature-dependent transmission for *Ae. aegypti* and *Ae. albopictus* that are (a) mechanistic, facilitating extrapolation beyond the current disease distribution, (b) parameterized with biologically accurate unimodal thermal responses for all mosquito and virus traits that drive transmission, and (c) validated against human dengue, chikungunya, and Zika case data across the Americas.

We synthesize available data to characterize the temperature-dependent traits of the mosquitoes and viruses that determine transmission intensity. With these thermal responses, we develop mechanistic temperature-dependent virus transmission models for *Ae. aegypti* and *Ae. albopictus*. We then ask whether the predicted effect of temperature on transmission is consistent with patterns of actual human cases over space and time. To do this, we validate the models with DENV, CHIKV, and ZIKV human incidence data at the country scale from the Americas from 2014-2016. To isolate temperature dependence, we also statistically controlled for population size and two socioeconomic factors that may influence transmission. If temperature fundamentally limits transmission potential, transmission should only occur at actual environmental temperatures that are predicted to be suitable, and conversely, areas with low predicted suitability should have low or zero transmission (i.e., false negative rates should be low). By contrast, low transmission may occur even when temperature suitability is high because other factors like vector control can limit transmission (i.e., the false positive rate should be higher than the false negative rate). Finally, if the simple mechanistic model accurately predicts

118 climate suitability for transmission, then we can use it to map climate-based transmission risk of
119 DENV, CHIKV, ZIKV, and other emerging pathogens transmitted by *Ae. aegypti* and *Ae.*
120 *albopictus* seasonally and geographically.

121 **Results**

122 *Temperature-dependent transmission*

123 Data gathered from the literature [9,13–15,15–21,21–30] revealed that all mosquito traits
124 relevant to transmission—biting rate, egg-to-adult survival and development rate, adult lifespan,
125 and fecundity—respond strongly to temperature and peak between 23°C and 34°C for the two
126 mosquito species (*Ae. aegypti* in Fig. 1 and *Ae. albopictus* in Fig. S1). DENV extrinsic
127 incubation and vector competence peak at 35°C [31–37] and 31-32°C [31,32,34,38],
128 respectively, in both mosquitoes—temperatures at which mosquito survival is low, limiting
129 transmission potential (Figs. 1, S1). Appropriate thermal response data were not available for
130 CHIKV and ZIKV extrinsic incubation and vector competence.

131

132 **Fig. 1.** Thermal responses of *Ae. aegypti* and DENV traits that drive transmission (data sources
133 listed in Table S2). Informative priors based on data from additional *Aedes* spp. and flavivirus
134 studies helped to constrain uncertainty in the model fits (see Materials and Methods; Table S3).
135 Points and error bars indicate the data means and standard errors (for display only; models were
136 fit from the raw data). Black solid lines are the mean model fits; red dashed lines are the 95%
137 credible intervals. Thermal responses for *Ae. albopictus* are shown in Fig. S1.

138

We estimated the posterior distribution of $R_0(T)$ and used it to calculate key temperature values that indicate suitability for transmission: the mean and 95% credible intervals (95% CI) on the critical thermal minimum, maximum, and optimum temperature for transmission by the two mosquito species. At constant temperature, *Ae. aegypti* transmission peaked at 29.1°C (95% CI: 28.4 – 29.8°C), and declined to zero below 17.8°C (95% CI: 14.6 – 21.2°C) and above 34.6°C (95% CI: 34.1 – 35.6°C) (Fig. 2). *Ae. albopictus* transmission peaked at 26.4°C (95% CI: 25.2 – 27.4°C) and declined to zero below 16.2°C (95% CI: 13.2 – 19.9°C) and above 31.6°C (95% CI: 29.4 – 33.7°C) (Fig. 2). Overall, the thermal response curve for *Ae. albopictus* is shifted towards lower temperatures than *Ae. aegypti,* so *Ae. albopictus* transmission is better suited to colder environments. For a more realistic scenario in which daily temperature ranged over 8°C, the transmission peak, minimum, and maximum were slightly lower for both *Ae. aegypti* (28.5°C, 13.5°C, 34.2°C, respectively) and *Ae. albopictus* (26.1°C, 11.9°C, and 28.3°C, respectively). The lower thermal maximum under fluctuating temperatures occurs because we incorporated empirically supported irreversible lethal effects of temperatures that exceed thermal maxima for survival (see Materials and Methods).

Fig. 2. Relative R_0 across constant temperatures (°C; top) for *Ae. albopictus* (light blue) and *Ae. aegypti* (dark blue), and histograms of the posterior distributions of the critical thermal minimum (bottom left), temperature at peak transmission (bottom middle), and critical thermal maximum (bottom right; all in °C). Solid lines: mean posterior estimates; dashed lines: 95% credible intervals. R_0 curves normalized to a 0-1 scale for ease of comparison and visualization.

The posterior distribution of $R_0(T)$ allows us to evaluate uncertainty in key temperature values that define the transmission range, including critical thermal minimum, maximum, and optimum. Uncertainty was higher for the critical thermal minimum for transmission than for the maximum or optimum, and the two mosquito species overlapped most for this outcome (Fig. 2, bottom panels). This occurred because several trait thermal responses increase gradually from low to mid temperatures but decline more steeply at high temperatures (Fig. 1), so uncertainty is greatest at low temperatures. *Ae. aegypti* has a substantially higher optimum and maximum temperature than *Ae. albopictus* (Fig. 2) due to its greater rates of adult survival at high temperatures (see Supplementary Materials for sensitivity analyses).

Model validation

We used generalized linear models (GLM) to ask whether the predicted relationship between temperature and transmission, $R_0(T)$, was consistent with observed human cases of DENV, CHIKV, and ZIKV. Specifically, we assessed whether $R_0(T)$ was an important predictor of the probability of autochthonous transmission occurring and of the incidence given that transmission occurred. We also controlled for human population size, virus species, and two socioeconomic factors. (Note that we focused on testing the $R_0(T)$ model, rather than on constructing the best possible statistical model of human case data.) To do this, we used the version of the *Ae. aegypti* $R_0(T)$ model that includes 8°C daily temperature range, along with country-scale weekly case reports of DENV, CHIKV, and ZIKV in the Americas and the Caribbean between 2014-2016. We first addressed the fact that countries with larger populations have greater opportunities for (large) epidemics by creating two predictors that incorporate scaled $R_0(T)$ and population size. In the models of the probability of autochthonous transmission

184 occurring we used the product of the posterior probability that $R_0(T) > 0$ (which we notate as
185 GR_0) and the log of population size (p) to give $log(p)*GR_0$. In the models of incidence given that
186 transmission does occur we used the log of the product of the posterior mean of $R_0(T)$ and
187 population size, $log(p*R_0(T))$. To control for several socioeconomic factors that might obscure
188 the impact of temperature, we also included log of gross domestic product (GDP) and log percent
189 of GDP in tourism (using logs to improve normality). These are potential indicators of
190 investment in and/or success of vector control and infrastructure improvements that prevent
191 transmission. By comparing models that included the $R_0(T)$ metric alone, socioeconomic factors
192 alone, or both, we tested whether $R_0(T)$ was an important predictor of observed transmission
193 occurrence and incidence (see Table S4). Note that $R_0(T)$ is out of sample because it is derived
194 and calculated strictly from laboratory data on mosquitoes, and we perform a validation analyses
195 for $R_0(T)$ using independent case incidence reports. For this validation step we assessed model
196 adequacy for the transmission data in two ways. First we used the full dataset for case incidence
197 reports to select the best model (Table S4) and determine whether or not our predicted value of
198 relative $R_0(T)$ based on laboratory data was included in the model ("within sample" analysis).
199 Second we used a bootstrapping approach where models were fit on subsets of the case incidence
200 data that were randomly sampled and then predictive accuracy of the competing models (Table
201 S4) was assessed on left-out data ("out of sample" analysis).

202 For the probability of autochthonous transmission occurring, the model that included both
203 the $R_0(T)$ predictor and socioeconomic predictors had overwhelming support based on Bayesian
204 Information Criterion (BIC; model PA5 relative probability = 1, Table S4). Based on deviance
205 explained, the models that included $R_0(T)$, with or without the socioeconomic predictors out-
206 performed the model that did not include $R_0(T)$ (Table S4; Figs. 3A, S2). In analyses of out-of-

sample accuracy, models that included the $R_0(T)$ metric (with or without the socioeconomic factors) were surprisingly accurate. They predicted the probability of transmission with 86-91% out-of-sample accuracy for DENV (Table S4). For CHIKV and ZIKV, models that included the $R_0(T)$ metric or population alone had 66-69% out-of-sample accuracy (Table S4). There were no significant differences in out-of-sample accuracy between the top four models but for both DENV and CHIKV/ZIKV the best model was significantly better than the worst model (see Supplementary Code for full results). The lower out-of-sample accuracy for CHIKV and ZIKV likely reflects the much lower frequency of positive values and the lower total sample size of this dataset. All results were similar for a set of models that separated GR_0 from population size, so for simplicity we show the model predictors that combines GR_0 and population size here (see Table S4 and Supplementary Code for results of other models). Further, from a biological perspective, the combined model better describes what we know about disease systems: if either the probability of $R_0(T)$ being greater than zero is small or population size is very small, transmission is unlikely to occur. Together, these analyses suggest that $R_0(T)$ is an important predictor of transmission occurrence, but that CHIKV and ZIKV need further data to better explain the probability of transmission occurrence (Figs. 3A, S2).

Fig. 3. *Ae. aegypti* $R_0(T)$ and population size predict the probability and magnitude of transmission of DENV, CHIKV, and ZIKV across the Americas. A, $log(p)*GR_0$ (the posterior probability that $R_0(T) > 0$ times the log of population size) versus the probability of local transmission in the data. B, $log(p*R_0(T))$ (log of $R_0(T)$ times the population size) versus the log of incidence, given that it exceeds the threshold for local transmission. Tick-marks and points: human transmission occurrence and incidence data, respectively, by country-week in the

Americas and Caribbean. Lines and shaded areas: mean and 95% CI from GLM fits for DENV (blue) and CHIKV and ZIKV (red). For simplicity, we show the models that only include the covariates $log(p)*GR_0$ or $log(p*R_0(T))$, respectively, and do not include the socioeconomic covariates (models PA6 and IM4 in Table S4). For each case report data point, $log(p)*GR_0$ and $log(p*R_0(T))$ were calculated at the mean temperature 10 weeks prior to the reporting week [39].

$R_0(T)$ was also an important predictor of incidence, given that autochthonous transmission did occur. Within-sample, incidence was best predicted by the model that included both $R_0(T)$ and the socioeconomic predictors (model IM5 in Table S4) based on BIC (relative probability = 1). The models that included $R_0(T)$ out-performed those that did not based on deviance explained (Table S4). In out-of-sample validation, the models that included $R_0(T)$ explained the magnitude of incidence based on mean absolute percentage error (85-86% accuracy versus 83% accuracy for models that did not include $R_0(T)$; Table S4), but this difference was not statistically significant. For illustration, we show the simpler model that only contains the $R_0(T)$ predictor in the main text (Fig. 3B; model IM1 in Table S4). Notably, the models that contained $R_0(T)$ predicted incidence well for all three viruses, despite the lower incidence of CHIKV and ZIKV.

Although predicted $R_0(T)$ correlated with the observed occurrence and magnitude of human incidence for all three viruses, these observed incidence metrics were higher for DENV than for CHIKV and ZIKV. While the reason for this difference is unclear, the most likely explanation is that DENV is much more established in the region, so it is more likely to be detected, diagnosed, and reported. Because ZIKV and CHIKV are newly emerging, they may not have fully saturated the region at this early stage.

253 The ability of the model to explain the probability and magnitude of transmission is
254 notable given the coarse scale of the human incidence versus mean temperature data (i.e.,
255 country-scale means), the lack of CHIKV- and ZIKV-specific trait thermal response data to
256 inform the model, the nonlinear relationship between transmission and incidence, and all the
257 well-documented factors other than temperature that influence transmission. Together, these
258 analyses show simple mechanistic models parameterized with laboratory data on mosquitoes and
259 dengue virus are consistent with observed temperature suitability for transmission. Moreover, the
260 similar responses of human incidence of ZIKV, CHIKV, and DENV to temperature suggest that
261 the thermal ecology of their shared mosquito vectors is a key determinant of outbreak location,
262 timing, and intensity.

263

264 *Mapping climate suitability for transmission*

265 The validated model can be used to predict where transmission is not excluded (posterior
266 probability that $R_0(T) > 0$, a conservative estimate of transmission risk). Considering the number
267 of months per year at which mean temperatures do not prevent transmission, large areas of
268 tropical and subtropical regions, including Puerto Rico and parts of Florida and Texas, are
269 currently suitable year-round or seasonally (Fig. 4). These regions are fundamentally at risk for
270 DENV, CHIKV, ZIKV, and other *Aedes* arbovirus transmission during a substantial part of the
271 year (Fig. 4). Indeed, DENV, CHIKV, and/or ZIKV local transmission has occurred in Texas,
272 Florida, Hawaii, and Puerto Rico (www.cdc.gov). On the other hand, many temperate regions
273 experience temperatures suitable for transmission three months or less per year (Fig. 4), and the
274 virus incubation periods in humans and mosquitoes restrict the transmission window even
275 further. Temperature thus limits the potential for the viruses to generate extensive epidemics in

276 temperate areas even where the vectors are present. Moreover, many temperate regions with
277 seasonally suitable temperatures currently lack *Ae. aegypti* and *Ae. albopictus* mosquitoes,
278 making vector transmission impossible (Fig. 4, black line). The posterior distribution of $R_0(T)$
279 also allows us to map months of risk with different degrees of uncertainty (e.g., 97.5%, 50%, and
280 2.5% posterior probability that that $R_0 > 0$), ranging from the most to least conservative (Fig.
281 S4).

282

283 **Fig. 4**. Map of predicted temperature suitability for virus transmission by *Ae. albopictus* and *Ae.*
284 *aegypti*. Color indicates the consecutive months in which temperature is permissive for
285 transmission (predicted $R_0 > 0$) for *Aedes* spp. transmission based on the minimum likely range
286 (> 97.5% posterior probability that $R_0 > 0$). Black lines indicate the CDC estimated range for the
287 two *Aedes* spp. in the United States. Model suitability predictions combine temperature mean
288 and 8°C daily variation and are informed by laboratory data (Figs. 1, S1) and validated against
289 field data (Fig. 3).

290

291 **Discussion**

292 Temperature is an important driver of—and limitation on—vector transmission, so
293 accurately describing the temperature range and optimum for transmission of DENV, CHIKV,
294 and ZIKV is critical for predicting their geographic and seasonal patterns of spread [12,40]. We
295 directly estimated the temperature – transmission relationship using mechanistic transmission
296 models for each mosquito species (Fig. 2). These models are built using empirical estimates of
297 the (unimodal) effects of temperature on mosquito and pathogen traits that drive transmission,
298 including survival, development, reproduction, and biting rates (Figs. 1, S1). Because these trait

thermal responses are unimodal across the majority of ectotherm taxa and traits, and because the traits combine nonlinearly to drive transmission, the emergent relationship between temperature and transmission is difficult to infer directly from field data or from individual trait responses. Here, we present a model of temperature-dependent DENV, CHIKV, and ZIKV transmission that advances on previous models because it is mechanistic, fitted from experimental trait data, and validated against independent human case data at a broad geographic scale (Fig. 3).

Mechanistic understanding is valuable for extrapolating beyond the current spatial and temporal range of transmission (Fig. 4), as compared to environmental niche models, for example [5,41,42]. Of the six previous mechanistic temperature-dependent models of DENV, CHIKV, or ZIKV transmission by *Ae. aegypti* and *Ae. albopictus* that we were able to reproduce, three had similar thermal optima [7,43,44] while the other three had dramatically higher optima (3-6°C) [9,45] (Fig. S5). Two models predicted much greater suitability for transmission at low temperatures [45], four predicted greater suitability at high temperatures [7,9,45], and two were very similar to ours [43,44] (Fig. S5). Only one of these previous models was (like ours) statistically validated against independent data not used to estimate model parameters, and its predictions were very similar to those of our model [43]. Other mechanistic and environmental niche models could not be directly compared with ours [5,10,40–42], either because fully reproducible equations, parameters, and/or code were not provided or because their predicted marginal effects of temperature were not displayed. Visually, our maps are similar to maps based on a previous model of *Ae. aegypti* and *Ae. albopictus* persistence suitability indices [40]. Recent environmental niche models of Zika distribution have shown similar but more constrained predicted distributions of environmental suitability, in part because these models include not just

321 temperature suitability but also further environmental, socioeconomic, and demographic
322 constraints [5,41,42,46].

323 Even though the thermal response data are imperfect—for example, CHIKV and ZIKV
324 thermal response data are missing—and the human case data are reported at a coarse spatial
325 scale, the validation analyses suggest that $R_0(T)$ is an important predictor of both the probability
326 of transmission occurring and the magnitude of incidence for DENV, CHIKV, and ZIKV. This
327 has several key implications. First, temperature-dependent transmission is pervasive enough to
328 be detected at a coarse spatial scale. Second, dynamics of the mosquito predict transmission for a
329 suite of *Ae. aegypti*-transmitted viruses, without additional virus-specific information. Third,
330 climate and socio-economic factors combine to shape variation in incidence across countries.
331 Finally, these simple predictors explain a substantial proportion of the variance in both the
332 probability and intensity of transmission.

333 Predicting arbovirus transmission at a higher spatial resolution and precision will require
334 more detailed information on factors like the exposure and susceptibility of human populations,
335 environmental variation (e.g., oviposition habitat availability, seasonal and daily temperature
336 variation), and socioeconomic factors. However, as a first step our mechanistic model provides
337 valuable insight because it makes broad predictions about suitable environmental conditions for
338 transmission, it is mechanistic and grounded in experimental trait data, it is validated against
339 independent human case data, and its predictions are applicable across three different viruses.
340 Using these thermal response models as a scaffold, additional drivers could be incorporated to
341 obtain more precise and specific predictions about transmission dynamics, which could in turn be
342 used for public health and vector control applications. For this purpose, all code and data used in
343 the models are available as Supplementary Files.

The socio-ecological conditions that enabled CHIKV, ZIKV, and DENV to become the three most important emerging vector-borne diseases in the Americas make the emergence of additional *Aedes*-transmitted viruses likely (potentially including Mayaro, Rift Valley fever, yellow fever, Uganda S, or Ross River viruses). Efforts to extrapolate and to map temperature suitability (Fig. 4) will be critical for improving management of both ongoing and future emerging epidemics. Mechanistic models like the one presented here are useful for extrapolating the potential geographic range of transmission beyond the current envelope of environmental conditions in which transmission occurs (e.g., under climate change and for newly invading pathogens). Accurately estimating temperature-driven transmission risk in both highly suitable and marginal regions is critical for predicting and responding to future outbreaks of these and other *Aedes*-transmitted viruses.

Materials and Methods

Temperature-sensitive R_0 models

We constructed temperature-dependent models of transmission using a previously developed R_0 framework. We modeled transmission rate as the basic reproduction rate, R_0—the number of secondary infections that would originate from a single infected individual introduced to a fully susceptible population. In previous work on malaria, we adapted a commonly used expression for R_0 for vector transmission to include the temperature-sensitive traits that drive mosquito population density :

$$R_0(T) = \left(\frac{a(T)^2\, b(T)\, c(T)\, e^{-\mu(T)/PDR(T)}\, EFD(T)\, p_{EA}(T)\, MDR(T)}{N\, r\, \mu(T)^3}\right)^{1/2} \quad (1)$$

Here, (T) indicates that the trait is a function of temperature, T; a is the per-mosquito biting rate, b is the proportion of infectious bites that infect susceptible humans, c is the proportion of bites

on infected humans that infect previously uninfected mosquitoes (i.e., $b*c$ = vector competence), μ is the adult mosquito mortality rate (lifespan, $lf = 1/\mu$), PDR is the parasite development rate (i.e., the inverse of the extrinsic incubation period, the time required between a mosquito biting an infected host and becoming infectious), EFD is the number of eggs produced per female mosquito per day, p_{EA} is the mosquito egg-to-adult survival probability, MDR is the mosquito immature development rate (i.e., the inverse of the egg-to-adult development time), N is the density of humans, and r is the human recovery rate. For each temperature-sensitive trait in each mosquito species, we fit either symmetric (Quadratic, $-c(T - T_0)(T - T_m)$) or asymmetric (Brière, $cT(T - T_0)(T_m - T)^{1/2}$) unimodal thermal response models to the available empirical data [47]. In both functions, T_0 and T_m are respectively the minimum and maximum temperature for transmission, and c is a positive rate constant.

We consider a normalized version of the R_0 equation such that it is rescaled to range from zero to one with the value of one occurring at the unimodal peak. Although absolute values of R_0 that are used to determine when transmission is stable depend on additional factors not captured in our model, the minimum and maximum temperatures for which $R_0 > 0$ map exactly onto our normalized equations, allowing us to accurately calculate whether or not transmission should be possible at all. Empirical estimates of absolute values of R_0 are difficult to obtain in any case, but it is much easier to determine whether transmission is occurring and for how long. While different model formulations for predicting R_0 versus temperature can produce results with different magnitudes and potentially different overall shapes [48], the temperatures for which R_0 is above or below zero (or one) are mostly model independent. For instance, two competing models differ only by whether or not the formula in equation (1) is squared, but the square of a number (e.g., an absolute R_0 value) greater than one is always greater than one, and the square of

a number less than one is always less than one. Therefore, the threshold temperatures at which absolute $R_0 > 0$ or absolute $R_0 > 1$ will be exactly the same for either choice of formula (Fig. S6). Similarly, because different expressions for R_0, including the square of equation (1), map monotonically onto our function, they will produce identical estimates for the temperatures at which transmission declines to zero and peaks (Fig. S6). Consequently, our use of relative R_0 adequately describes the nonlinear relationship between mosquito and virus traits and transmission.

We fit the trait thermal responses in equation (1) based on an exhaustive search of published laboratory studies that fulfilled the criterion of measuring a trait at three or more constant temperatures, ideally capturing both the rise and the fall of each unimodal curve (Tables S1-S2). Constant-temperature laboratory conditions are required to isolate the direct effect of temperature from confounding factors in the field and to provide a baseline for estimating the effects of temperature variation through rate summation [49]. We attempted to obtain raw data from each study, but if they were not available we collected data by hand from tables or digitized data from figures using WebPlotDigitizer [50]. We obtained raw data from Delatte [19] and Alto [21] for the *Ae. albopictus* egg-to-adult survival probability (*pEA*), mosquito development rate (MDR), gonotrophic cycle duration (GCD, which we assumed was equal to the inverse of the biting rate) and total fecundity (TFD) (Table S2). Data did not meet the inclusion criterion for CHIKV or ZIKV vector competence (*b, c*) or extrinsic incubation period (*EIP*) in either *Ae. albopictus* or *Ae. aegypti*. Instead, we used DENV EIP and vector competence data, combined with sensitivity analyses.

Following Johnson *et al.* [51], we fit a thermal response for each trait using Bayesian models. We first fit Bayesian models for each trait thermal response using uninformative priors

412 (T_0 ~ Uniform (0, 24), T_m ~ Uniform (25, 45), c ~ Gamma (1, 10) for Brière and c ~ Gamma (1,
413 1) for Quadratic fits) chosen to restrict each parameter to its biologically realistic range (i.e., T_0 <
414 T_m and we assumed that temperatures below 0°C and above 45°C were lethal). Any negative
415 values for all thermal response functions were truncated at zero, and thermal responses for
416 probabilities (p_{EA}, b, and c) were also truncated at one. We modeled the observed data as arising
417 from a normal distribution with the mean predicted by the thermal response function calculated
418 at the observed temperature, and the precision τ, ($\tau = 1/\sigma$), distributed as τ ~ Gamma (0.0001,
419 00001). We fit the models using Markov Chain Monte Carlo (MCMC) sampling in JAGS, using
420 the R [52] package *rjags* [53]. For each thermal response, we ran five MCMC chains with a
421 5000-step burn-in and saved the subsequent 5000 steps. We thinned the posterior samples by
422 saving every fifth sample and used the samples to calculate R_0 from 15-40°C, producing a
423 posterior distribution of R_0 versus temperature. We summarized the relationship between
424 temperature and each trait or overall R_0 by calculating the mean and 95% highest posterior
425 density interval (HPD interval; a type of credible interval that includes the smallest continuous
426 range containing 95% of the probability, as implemented in the *coda* package [54]) for each
427 curve across temperatures.

428 We fit a second set of models for each mosquito species that used informative priors to
429 reduce uncertainty in R_0 versus temperature and in the trait thermal responses. In these models,
430 we used Gamma-distributed priors for each parameter T_0, T_m, c, and τ fit from an additional
431 'prior' dataset of *Aedes* spp. trait data that did not meet the inclusion criteria for the primary
432 dataset (Table S3). We found that these initial informative priors could have an overly strong
433 influence on the posteriors, in some cases drawing the posterior distributions well away from the
434 primary dataset, which was better controlled and met the inclusion criteria. We accounted for our

lower confidence in this data set by increasing the variance in the informative priors, by multiplying all hyperparameters (i.e., the parameters of the Gamma distributions of priors for T_0, T_m, and c) by a constant k to produce a distribution with the same mean but $1/k$ times larger variance. We chose the value of k based on our relative confidence in the prior versus main data. Thus we chose $k = 0.5$ for *b, c,* and *PDR* and $k = 0.01$ for *lf*. This is the main model presented in the text (Fig. 2). It is comparable to some but not all previous mechanistic models for *Ae. aegypti* and *Ae. albopictus* transmission (Fig. S5). Results of our main model, fit with informative priors, did not vary substantially from the model fit with uninformative priors (Figs. S7-S8).

Incorporating daily temperature variation in transmission models

Because organisms do not typically experience constant temperature environments in nature, we incorporated the effects of temperature variation on transmission by calculating a daily average R_0 assuming a daily temperature range of 8°C, across a range of mean temperatures. This range is consistent with daily temperature variation in tropical and subtropical environments but lower than in most temperate environments. At each mean temperature, we used a Parton-Logan model to generate hourly temperatures and calculate each temperature-sensitive trait on an hourly basis [55]. We assumed an irreversible high-temperature threshold above which mosquitoes die and transmission is impossible [56,57]. We set this threshold based on hourly temperatures exceeding the critical thermal maximum (T_m in Tables S1-S2) for egg-to-adult survival or adult longevity by any amount for five hours or by 3°C for one hour. We averaged each trait over 24 hours to obtain a daily average trait value, which we used to calculate relative R_0 across a range of mean temperatures. We used this model in the validation against human cases (Fig. 3) and the risk map (Fig. 4).

Model validation with DENV, CHIKV, and ZIKV incidence data

458 To validate the model, we used data on human cases of DENV, CHIKV, and ZIKV at the
459 country scale and mean temperature during the transmission window. Using statistical models
460 (as described below), we estimated the effects of predicted $R_0(T)$ on the probability of local
461 transmission and the magnitude of incidence, controlling for population size and several
462 socioeconomic factors. We downloaded and manually entered Pan American Health
463 Organization (PAHO) weekly case reports for DENV and CHIKV for all countries in the
464 Americas (North, Central, and South America and the Caribbean Islands) from week 1 of 2014
465 to week 8 of 2015 for CHIKV and from week 52 of 2013 to week 47 of 2015 for DENV
466 (www.paho.org). ZIKV weekly case reports for reporting districts (e.g., provinces) within
467 Colombia, Mexico, El Salvador, and the US Virgin Islands were available from the CDC
468 Epidemic Prediction Initiative (https://github.com/cdcepi/) from November 28, 2015 to April 2,
469 2016. We aggregated the ZIKV data into country-level weekly case reports to match the spatial
470 resolution of the DENV, CHIKV, and covariate data.

471

472 Temperature data collection

473 We matched the DENV, CHIKV, and ZIKV incidence data with temperature using daily
474 temperature data from METAR stations in each country, averaged at the country level by
475 epidemic week. A previous study found a six-week lagged relationship between temperature and
476 oviposition for *Aedes aegypti* in Ecuador [39]. Assuming that the subsequent transmission,
477 disease development, medical care-seeking, and case reporting in humans takes an additional
478 four weeks, we assumed *a priori* a ten-week lag between temperature and incidence (i.e., mean
479 temperature for the week that is ten weeks prior to each case report). METAR stations are
480 internationally standardized weather reporting stations that report hourly temperature and

481 precipitation measures. Outlier weather stations were excluded if they reported a daily maximum
482 temperature below 5°C or a daily minimum temperature above 40°C during the study period,
483 extremes that would certainly eliminate the potential for transmission in a local area. Because
484 case data are reported at the country level, we needed a collection of weather stations in each
485 country that accurately represent weather conditions in the areas where transmission occurs,
486 excluding extreme areas where transmission is unlikely. For the study period of October 1, 2013
487 through April 30, 2016, we downloaded daily temperature data for each station from Weather
488 Underground using the *weatherData* package in R [58]. We removed all data from Chile because
489 it spans so much latitude and the terrain is so diverse that its country-level mean is unlikely to be
490 very representative of the temperature where an outbreak occurred.

491 Socioeconomic covariate data

492 We accessed available data on projected 2016 gross domestic product (GDP) for
493 countries of interest via the International Monetary Fund's World Economic Outlook Database
494 (http://www.imf.org/external/ns/cs.aspx?id=28). The direct and total contributions of tourism to
495 GDP in 2016 were compiled from World Travel and Tourism Council economic impact reports
496 (http://www.wttc.org/research/economic-research/economic-impact-analysis/country-
497 reports/#undefined). We retrieved population size data for 2013-2015 from the United Nations
498 Population Division (https://esa.un.org/unpd/wpp/Download/Standard/Population/) and averaged
499 them across the three years for each country. Throughout the analyses below, unless otherwise
500 specified, we used the natural log of the population size and of GDP as our predictors. We have
501 two reasons for this choice. The first is that, intuitively, the relative order of magnitude of the
502 population/GDP is more important in determining observed outbreak sizes or probabilities than
503 their absolute sizes. Second, population sizes and GDPs across countries tend to exhibit clumped

patterns with a few outliers that are much larger than the others. From a statistical perspective, using the un-transformed populations (or GDPs) results in those few large/rich countries having very high leverage in the analysis, and thus potentially skewing the results. Taking a log of the population better balances these predictors and is the standard accepted approach when using these kinds of predictors in regression models.

Validation analyses with human incidence versus temperature datasets

To validate the $R_0(T)$ model while controlling for population and socio-economic factors, we used generalized linear regression on the weekly case count data. Importantly, we focused on testing whether the case counts were consistent with the transmission – temperature relationship predicted from our model, rather than on maximizing the variation explained in the statistical model. We are more specifically interested in understanding autochthonous transmission (i.e., locally acquired, not just imported cases). We set country-level thresholds for the number of cases defining autochthonous transmission for our three diseases separately, based on current transmission understanding: seven cases of CHIKV, 70 cases of DENV, and three cases of ZIKV. We derived these thresholds in the following way. First, we looked for data on outbreaks of travel related cases in countries that are not expected to experience any local transmission. For instance, in 2014 Canada experienced 320 confirmed, travel-related cases of chikungunya (http://www.phac-aspc.gc.ca/publicat/ccdr-rmtc/15vol41/dr-rm41-01/rapid-eng.php), equivalent to an average of more than six cases per week. Thus, to be conservative in our estimates, we set the threshold of transmission as seven cases/week for CHIKV. The reported weekly cases of DENV transmission in our study sample are considerably higher than for CHIKV (mean DENV incidence was nearly 100 times higher mean CHIKV incidence). We chose a moderately high threshold of 70 cases in a week (i.e., 10 times higher than the CHIKV threshold based on

Canadian cases) to reflect higher overall incidence and increased potential for travel related cases. We examined the sensitivity of the results to choice of threshold by varying it from 25 to 100, and we found qualitatively similar results for all thresholds that we tested. As ZIKV is not as well established as either CHIKV or DENV at this time, smaller numbers of cases may indicate autochthonous transmission. Consequently, we chose a threshold of three cases for ZIKV (approximately half the CHIKV threshold). Further, the results were fairly sensitive to the ZIKV threshold as many locations have small numbers of cases. Since higher thresholds exclude a very large proportion of available case data making analysis impossible, we used the slightly less conservative threshold of three cases for autochthonous transmission of ZIKV. The resulting data consisted of zeros for no transmission and positive case counts when transmission is presumed to be occurring. To model these data, we used a hurdle model that first uses logistic regression on the presence/absence of local transmission data to understand the factors correlated with local transmission occurring or not (PA analysis). Then we modeled the log of incidence (number of new cases per reporting week) for positive values with a gamma generalized linear models (GLM; i.e., incidence analysis).

We were interested in understanding whether $R_0(T)$ was an important predictor of human transmission occurrence and incidence, after controlling for potentially confounding factors like population size and socioeconomic conditions. To do this, we fit a series of models with different subsets of predictors that included $R_0(T)$, the socioeconomic variables with population, or both (see Table S4 for full models). To control for human population size, we created new metrics based on $R_0(T)$ and population size to use for validation against the PAHO incidence data. We define GR_0, which is the posterior probability that $R_0(T) > 0$. We use $log(p)*GR_0$, where p is the population size, as the relevant R_0-based predictor for the PA analysis. For the incidence

550 analysis, we instead use $log(p*R_0(T))$ as the predictor. In all cases log refers to the natural
551 logarithm. For simplicity, we refer to these as the $R_0(T)$ metrics hereafter and in the Results.

552 In both the PA and incidence analyses, we first used the full data sets to examine which
553 of the candidate models best described the data. Randomized quantile residuals indicated that the
554 logistic and gamma GLM models were performing adequately. We compared the approximate
555 model probabilities, calculated from the BIC scores, as well as the proportion of deviance
556 explained (D^2) from each model. Next we examined the performance of the models in predicting
557 out of sample, for both PA and incidence analyses. To do this we created 1000 random
558 partitions, where 90% of the data were used to train the model and 10% were used for testing. In
559 the PA analyses we classified each partition based on presence/absence, with separate
560 classification thresholds for DENV versus CHIKV/ZIKV as these grouping had much different
561 probabilities of occurrence. We assessed the performance of the model for the PA analysis based
562 on the mean misclassification rate. In the incidence analyses we assessed the model performance
563 based on the predictive mean absolute percentage error (MAPE). Since differences in prediction
564 success between the models in both the PA and incidence analyses were not statistically
565 significant, we present the simpler models that only include the $R_0(T)$ metrics in the main text
566 (Fig. 3) and the models that additionally include socioeconomic covariates in the Supplementary
567 Information (Figs. S2-S3). We plotted the model predictions as a function of the $R_0(T)$ metrics
568 together with the observed data for the PA and incidence analyses using the R package *visreg*
569 [59].

570 The residuals of the incidence model exhibit "inverse trumpeting," in which residual
571 variation is larger at low than high predicted incidence (Fig. S9). This occurs in part because we
572 forced the model to go through the origin, i.e., no transmission when $R_0(T)$ or the population size

573 is equal to zero. However, the data did sometimes show transmission where we did not expect it,
574 potentially because of imported cases, errors in reporting, or small pockets of transmission
575 suitability in countries or times that are otherwise unsuitable on average. More local-scale case
576 reporting that separates autochthonous from travel-associated cases would be needed to tease
577 apart the source of this error.

578

579 Mapping temperature suitability for transmission

580 Using our validated model, we were interested in where the temperature was suitable for
581 *Ae. aegypti* and/or *Ae. albopictus* transmission for some or all of the year to predict the potential
582 geographic range of outbreaks in the Americas. We visualized the minimum, median, and
583 maximum extent of transmission based on probability of occurrence thresholds from the R_0
584 models for both mosquitoes. We calculated the number of consecutive months in which the
585 posterior probability of $R_0 > 0$ exceeds a threshold of 0.025, 0.5, or 0.975 for both mosquito
586 species, representing the maximum, median, and minimum likely ranges, respectively. The
587 minimum range is shown in Fig. 4 and all three ranges are overlaid in Fig. S4. This analysis
588 indicates the predicted seasonality of temperature suitability for transmission geographically, but
589 does not indicate its magnitude. To generate the maps, we cropped monthly mean temperature
590 rasters from 1950-2000 for all twelve months (Worldclim; www.worldclim.org/) to the Americas
591 (*R*, *raster* package, *crop* function) and assigned cells values of one or zero depending on whether
592 the probability that $R_0 > 0$ exceeded the threshold at the temperatures in those cells. We then
593 synthesized the monthly grids into a single raster that reflected the maximum number of
594 consecutive months where cell values equaled one. The resulting rasters were plotted in ArcGIS
595 10.3, overlaying the three cutoffs (Fig. S4). We repeated this process for both mosquito species.

596

597

598 **Acknowledgments**

599 Barry Alto, Krijn Paaijmans, Francis Ezeakacha, and Helene Delatte kindly provided raw data
600 used in the analyses. We gratefully acknowledge the Centers for Disease Control and Prevention
601 Epidemic Predictions Initiative (CDC EPI) for collating and sharing the Zika incidence data on
602 GitHub (https://zenodo.org/record/48946#.Vz-EM2bb8ys).

603

604 **Supporting Information Legends**

605 **S1 Appendix. Supplementary Results, References, Figures S1-S15, and Tables S1-S3.**

606 **S2 Appendix. Table S4.** Model validation results.

607 **S3 Appendix. Online code, data, and analyses.** Available as a ZIP file on Figshare:
608 https://figshare.com/s/b79bc7537201e7b5603f, DOI:
609 https://dx.doi.org/10.6084/m9.figshare.4563928.

610

References:

1. Brady OJ, Gething PW, Bhatt S, Messina JP, Brownstein JS, Hoen AG, et al. Refining the global spatial limits of dengue virus transmission by evidence-based consensus. PLOS Negl Trop Dis. 2012;6: e1760. doi:10.1371/journal.pntd.0001760

2. Bhatt S, Gething PW, Brady OJ, Messina JP, Farlow AW, Moyes CL, et al. The global distribution and burden of dengue. Nature. 2013;496: 504–507. doi:10.1038/nature12060

3. Rasmussen SA, Jamieson DJ, Honein MA, Petersen LR. Zika virus and birth defects — reviewing the evidence for causality. N Engl J Med. 2016;374: 1981–1987. doi:10.1056/NEJMsr1604338

4. Scott TW, Takken W. Feeding strategies of anthropophilic mosquitoes result in increased risk of pathogen transmission. Trends Parasitol. 2012;28: 114–121. doi:10.1016/j.pt.2012.01.001

5. Messina JP, Kraemer MU, Brady OJ, Pigott DM, Shearer FM, Weiss DJ, et al. Mapping global environmental suitability for Zika virus. eLife. 2016;5: e15272. doi:10.7554/eLife.15272

6. Magori K, Legros M, Puente ME, Focks DA, Scott TW, Lloyd AL, et al. Skeeter Buster: A stochastic, spatially explicit modeling tool for studying Aedes aegypti population replacement and population suppression strategies. PLOS Negl Trop Dis. 2009;3: e508. doi:10.1371/journal.pntd.0000508

7. Johansson MA, Powers AM, Pesik N, Cohen NJ, Staples JE. Nowcasting the spread of chikungunya virus in the Americas. PLoS ONE. 2014;9: e104915. doi:10.1371/journal.pone.0104915

8. Perkins TA, Metcalf CJE, Grenfell BT, Tatem AJ. Estimating drivers of autochthonous transmission of chikungunya virus in its invasion of the Americas. PLoS Curr. 2015;7. doi:10.1371/currents.outbreaks.a4c7b6ac10e0420b1788c9767946d1fc

9. Morin CW, Monaghan AJ, Hayden MH, Barrera R, Ernst K. Meteorologically driven simulations of dengue epidemics in San Juan, PR. PLoS Negl Trop Dis. 2015;9: e0004002. doi:10.1371/journal.pntd.0004002

10. Zhang Q, Sun K, Chinazzi M, Pastore-Piontti A, Dean NE, Rojas DP, et al. Projected spread of Zika virus in the Americas. bioRxiv. 2016; 066456. doi:10.1101/066456

11. Dell AI, Pawar S, Savage VM. Systematic variation in the temperature dependence of physiological and ecological traits. Proc Natl Acad Sci. 2011;108: 10591–10596.

12. Mordecai EA, Paaijmans KP, Johnson LR, Balzer CH, Ben-Horin T, de Moor E, et al. Optimal temperature for malaria transmission is dramatically lower than previously predicted. Ecol Lett. 2013;16: 22–30.

13. Focks DA, Haile DG, Daniels E, Mount GA. Dynamic life table model for Aedes aegypti (Diptera: Culicidae): analysis of the literature and model development. J Med Entomol. 1993;30: 1003–1017.

14. Yang HM, Macoris MLG, Galvani KC, Andrighetti MTM, Wanderley DMV. Assessing the effects of temperature on the population of Aedes aegypti, the vector of dengue. Epidemiol Infect. 2009;137: 1188–1202. doi:10.1017/S0950268809002040

15. Rueda L, Patel K, Axtell R, Stinner R. Temperature-dependent development and survival rates of Culex quinquefasciatus and Aedes aegypti (Diptera: Culicidae). J Med Entomol. 1990;27: 892–898.

16. Tun-Lin W, Burkot TR, Kay BH. Effects of temperature and larval diet on development rates and survival of the dengue vector Aedes aegypti in north Queensland, Australia. Med Vet Entomol. 2000;14: 31–37. doi:10.1046/j.1365-2915.2000.00207.x

649 17. Kamimura K, Matsuse IT, Takahashi H, Komukai J, Fukuda T, Suzuki K, et al. Effect of temperature on the
650 development of Aedes aegypti and Aedes albopictus. Med Entomol Zool. 2002;53: 53–58.

651 18. Eisen L, Monaghan AJ, Lozano-Fuentes S, Steinhoff DF, Hayden MH, Bieringer PE. The impact of
652 temperature on the bionomics of Aedes (Stegomyia) aegypti, with special reference to the cool geographic
653 range margins. J Med Entomol. 2014;51: 496–516. doi:10.1603/ME13214

654 19. Delatte H, Gimonneau G, Triboire A, Fontenille D. Influence of temperature on immature development,
655 survival, longevity, fecundity, and gonotrophic cycles of Aedes albopictus, vector of chikungunya and dengue
656 in the Indian Ocean. J Med Entomol. 2009;46: 33–41. doi:10.1603/033.046.0105

657 20. Muturi EJ, Lampman R, Costanzo K, Alto BW. Effect of temperature and insecticide stress on life-history traits
658 of Culex restuans and Aedes albopictus (Diptera: Culicidae). J Med Entomol. 2011;48: 243–250.

659 21. Alto BW, Juliano SA. Temperature effects on the dynamics of Aedes albopictus (Diptera: Culicidae)
660 populations in the laboratory. J Med Entomol. 2001;38: 548–556.

661 22. Westbrook CJ, Reiskind MH, Pesko KN, Greene KE, Lounibos LP. Larval environmental temperature and the
662 susceptibility of Aedes albopictus Skuse (Diptera: Culicidae) to chikungunya virus. Vector-Borne Zoonotic
663 Dis. 2010;10: 241–247. doi:10.1089/vbz.2009.0035

664 23. Briegel H, Timmermann SE. Aedes albopictus (Diptera: Culicidae): Physiological aspects of development and
665 reproduction. J Med Entomol. 2001;38: 566–571. doi:10.1603/0022-2585-38.4.566

666 24. Calado DC, Navarro-Silva MA. Influência da temperatura sobre a longevidade, fecundidade e atividade
667 hematofágica de Aedes (Stegomyia) albopictus Skuse, 1894 (Diptera, Culicidae) sob condições de laboratório.
668 Rev Bras Entomol. 2002;46: 93–98. doi:10.1590/S0085-56262002000100011

669 25. Beserra EB, Fernandes CRM, Silva SA de O, Silva LA da, Santos JW dos. Efeitos da temperatura no ciclo de
670 vida, exigências térmicas e estimativas do número de gerações anuais de Aedes aegypti (Diptera, Culicidae).
671 Iheringia Sér Zool. 2009; Available: http://agris.fao.org/agris-search/search.do?recordID=XS2010500501

672 26. Westbrook CJ. Larval ecology and adult vector competence of invasive mosquitoes Aedes albopictus and
673 Aedes aegypti for Chikungunya virus [Internet]. University of Florida. 2010. Available:
674 http://etd.fcla.edu/UF/UFE0041830/westbrook_c.pdf

675 27. Couret J, Dotson E, Benedict MQ. Temperature, Larval Diet, and Density Effects on Development Rate and
676 Survival of Aedes aegypti (Diptera: Culicidae). PLoS ONE. 2014;9: e87468.
677 doi:10.1371/journal.pone.0087468

678 28. Ezeakacha N. Environmental impacts and carry-over effects in complex life cycles: the role of different life
679 history stages. Dissertation. 2015; Available: http://aquila.usm.edu/dissertations/190

680 29. Teng H-J, Apperson CS. Development and Survival of Immature Aedes albopictus and Aedes triseriatus
681 (Diptera: Culicidae) in the Laboratory: Effects of Density, Food, and Competition on Response to
682 Temperature. J Med Entomol. 2000;37: 40–52. doi:10.1603/0022-2585-37.1.40

683 30. Wiwatanaratanabutr S, Kittayapong P. Effects of temephos and temperature on Wolbachia load and life history
684 traits of Aedes albopictus. Med Vet Entomol. 2006;20: 300–307. doi:10.1111/j.1365-2915.2006.00640.x

685 31. Xiao F-Z, Zhang Y, Deng Y-Q, He S, Xie H-G, Zhou X-N, et al. The effect of temperature on the extrinsic
686 incubation period and infection rate of dengue virus serotype 2 infection in Aedes albopictus. Arch Virol.
687 2014;159: 3053–3057. doi:10.1007/s00705-014-2051-1

32. Watts DM, Burke DS, Harrison BA, Whitmire RE, Nisalak A. Effect of temperature on the vector efficiency of Aedes aegypti for dengue 2 virus. Am J Trop Med Hyg. 1987;36: 143–152.

33. McLean DM, Clarke AM, Coleman JC, Montalbetti CA, Skidmore AG, Walters TE, et al. Vector capability of Aedes aegypti mosquitoes for California encephalitis and dengue viruses at various temperatures. Can J Microbiol. 1974;20: 255–262. doi:10.1139/m74-040

34. Carrington LB, Armijos MV, Lambrechts L, Scott TW. Fluctuations at a low mean temperature accelerate dengue virus transmission by Aedes aegypti. PLoS Negl Trop Dis. 2013;7: e2190. doi:10.1371/journal.pntd.0002190

35. Davis NC. The effect of various temperatures in modifying the extrinsic incubation period of the yellow fever virus in Aedes aegypti. Am J Epidemiol. 1932;16: 163–176.

36. McLean DM, Miller MA, Grass PN. Dengue virus transmission by mosquitoes incubated at low temperatures. Mosq News. 1975; Available: http://agris.fao.org/agris-search/search.do?recordID=US19760088008

37. Focks DA, Daniels E, Haile DG, Keesling JE. A simulation model of the epidemiology of urban dengue fever: literature analysis, model development, preliminary validation, and samples of simulation results. Am J Trop Med Hyg. 1995;53: 489–506.

38. Alto BW, Bettinardi D. Temperature and dengue virus infection in mosquitoes: independent effects on the immature and adult stages. Am J Trop Med Hyg. 2013;88: 497–505. doi:10.4269/ajtmh.12-0421

39. Stewart Ibarra AM, Ryan SJ, Beltrán E, Mejía R, Silva M, Muñoz Á. Dengue vector dynamics (Aedes aegypti) influenced by climate and social factors in Ecuador: implications for targeted control. PLoS ONE. 2013;8: e78263. doi:10.1371/journal.pone.0078263

40. Brady OJ, Golding N, Pigott DM, Kraemer MUG, Messina JP, Reiner Jr RC, et al. Global temperature constraints on Aedes aegypti and Ae. albopictus persistence and competence for dengue virus transmission. Parasit Vectors. 2014;7: 338. doi:10.1186/1756-3305-7-338

41. Carlson CJ, Dougherty ER, Getz W. An Ecological Assessment of the Pandemic Threat of Zika Virus. PLoS Negl Trop Dis. 2016;10: e0004968. doi:10.1371/journal.pntd.0004968

42. Samy AM, Thomas SM, Wahed AAE, Cohoon KP, Peterson AT, Samy AM, et al. Mapping the global geographic potential of Zika virus spread. Mem Inst Oswaldo Cruz. 2016;111: 559–560. doi:10.1590/0074-02760160149

43. Wesolowski A, Qureshi T, Boni MF, Sundsøy PR, Johansson MA, Rasheed SB, et al. Impact of human mobility on the emergence of dengue epidemics in Pakistan. Proc Natl Acad Sci. 2015; 201504964. doi:10.1073/pnas.1504964112

44. Liu-Helmersson J, Stenlund H, Wilder-Smith A, Rocklöv J. Vectorial Capacity of Aedes aegypti: Effects of Temperature and Implications for Global Dengue Epidemic Potential. PLoS ONE. 2014;9: e89783. doi:10.1371/journal.pone.0089783

45. Caminade C, Turner J, Metelmann S, Hesson JC, Blagrove MSC, Solomon T, et al. Global risk model for vector-borne transmission of Zika virus reveals the role of El Niño 2015. Proc Natl Acad Sci. 2017;114: 119–124. doi:10.1073/pnas.1614303114

46. Bogoch II, Brady OJ, Kraemer MUG, German M, Creatore MI, Kulkarni MA, et al. Anticipating the international spread of Zika virus from Brazil. The Lancet. 2016;387: 335–336. doi:10.1016/S0140-6736(16)00080-5

728 47. Briere J-F, Pracros P, Le Roux A-Y, Pierre J-S. A novel rate model of temperature-dependent development for
729 arthropods. Environ Entomol. 1999;28: 22–29.

730 48. Li J, Blakeley D, Smith? RJ. The Failure of *R*0. Comput Math Methods Med. 2011;2011: e527610.
731 doi:10.1155/2011/527610

732 49. Lambrechts L, Paaijmans KP, Fansiri T, Carrington LB, Kramer LD, Thomas MB, et al. Impact of daily
733 temperature fluctuations on dengue virus transmission by Aedes aegypti. Proc Natl Acad Sci. 2011;108:
734 7460–7465. doi:10.1073/pnas.1101377108

735 50. Rohatgi A. WebPlotDigitizer [Internet]. 2015. Available: http://arohatgi.info/WebPlotDigitizer

736 51. Johnson LR, Ben-Horin T, Lafferty KD, McNally A, Mordecai E, Paaijmans KP, et al. Understanding
737 uncertainty in temperature effects on vector-borne disease: a Bayesian approach. Ecology. 2015;96: 203–213.
738 doi:10.1890/13-1964.1

739 52. R Development Core Team. R: A Language and Environment for Statistical Computing [Internet]. Vienna,
740 Austria: R Foundation for Statistical Computing; 2014. Available: http://www.R-project.org

741 53. Plummer M. rjags: Bayesian Graphical Models using MCMC [Internet]. 2016. Available: http://CRAN.R-
742 project.org/package=rjags

743 54. Plummer M, Best N, Cowles K, Vines K. CODA: Convergence Diagnosis and Output Analysis for MCMC.
744 2006.

745 55. Parton WJ, Logan JA. A model for diurnal variation in soil and air temperature. Agric Meteorol. 1981;23: 205–
746 216. doi:10.1016/0002-1571(81)90105-9

747 56. Paaijmans KP, Heinig RL, Seliga RA, Blanford JI, Blanford S, Murdock CC, et al. Temperature variation
748 makes ectotherms more sensitive to climate change. Glob Change Biol. 2013;19: 2373–2380.
749 doi:10.1111/gcb.12240

750 57. Vasseur DA, DeLong JP, Gilbert B, Greig HS, Harley CDG, McCann KS, et al. Increased temperature variation
751 poses a greater risk to species than climate warming. Proc R Soc Lond B Biol Sci. 2014;281: 20132612.
752 doi:10.1098/rspb.2013.2612

753 58. Narasimhan R. weatherData: Get Weather Data from the Web [Internet]. 2014. Available: https://cran.r-
754 project.org/web/packages/weatherData/index.html

755 59. Breheny P, Burchett W. visreg: Visualization of Regression Models [Internet]. 2016. Available: https://cran.r-
756 project.org/web/packages/visreg/index.html

757

758

759 **Figure 1**

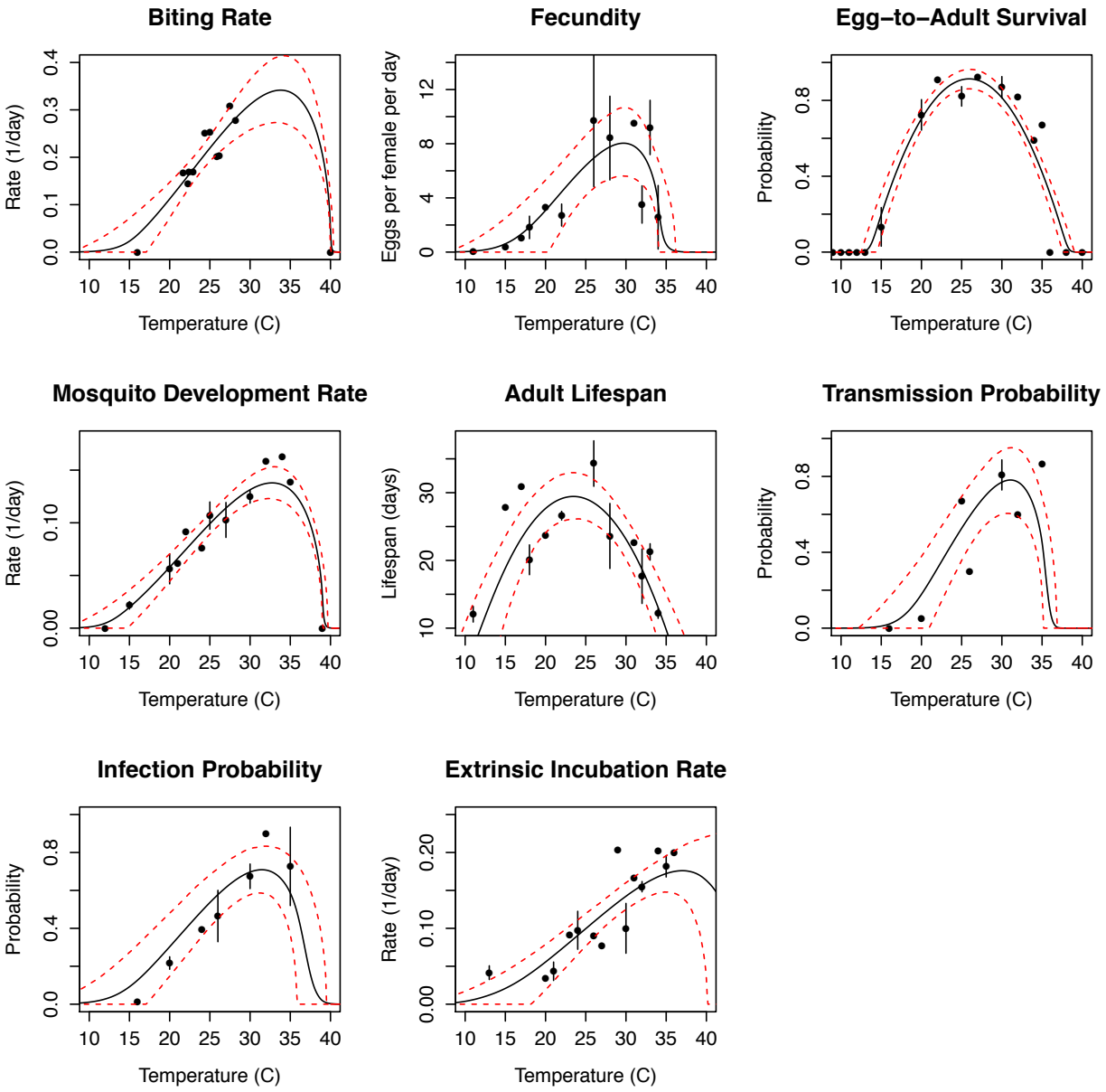

760

761

762 **Figure 2**

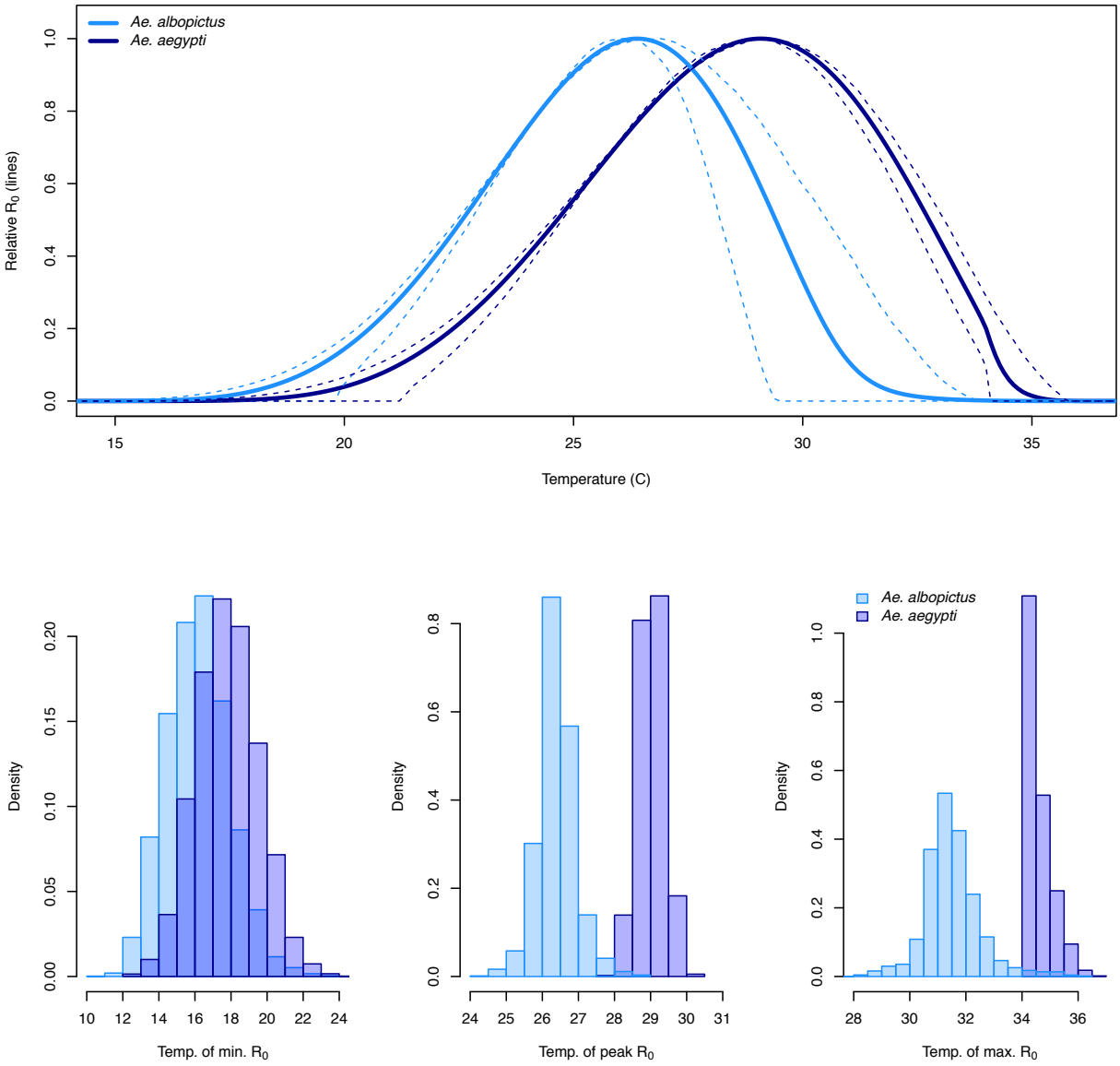

763

764

765 **Figure 3**

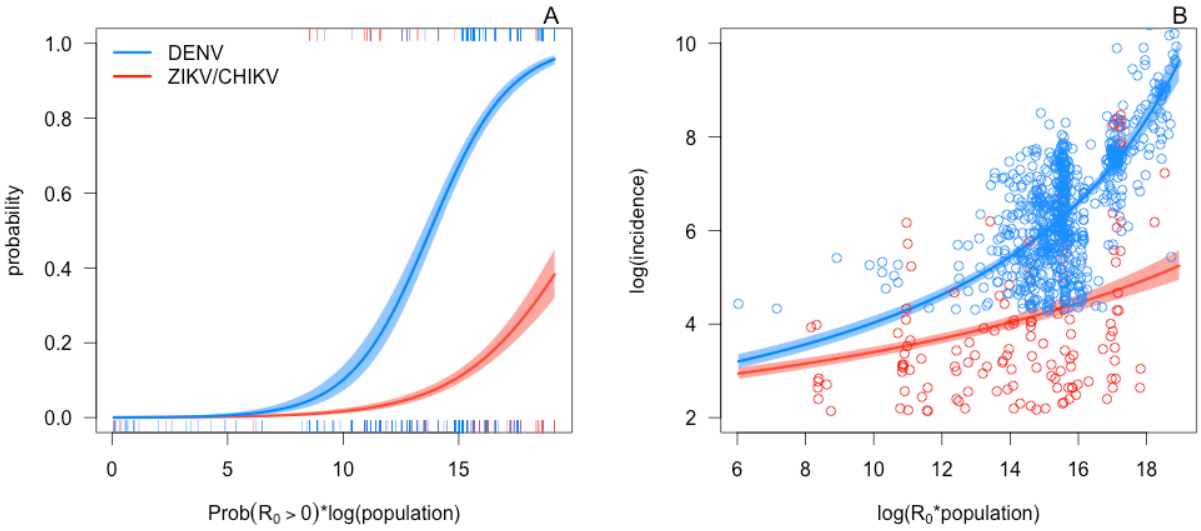

766

767

768 **Figure 4**

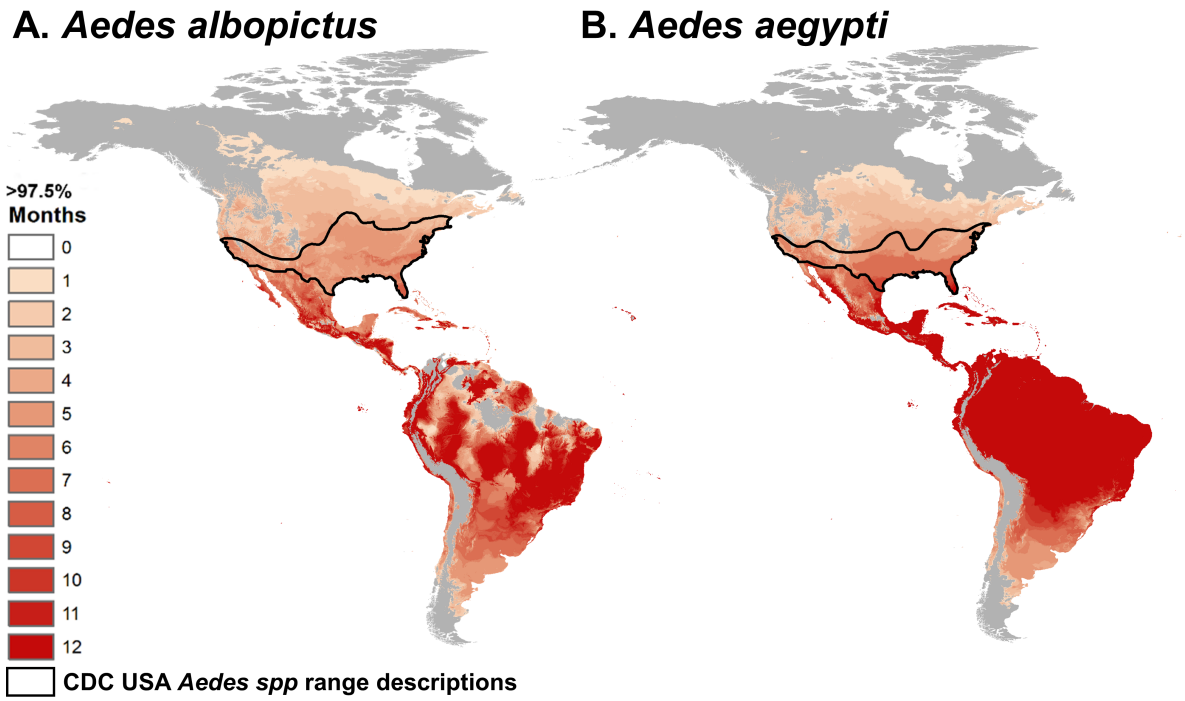

769